COMSOL
CONFERENCE
2024 FLORENCE

# Geological carbon storage: a FEM reactive transport model to assess caprock degradation

L. Gramegna[1], G. Volontè[2], G. Della Vecchia[1]
1. Department of Civil and Environmental Engineering, Politecnico di Milano, Milano, Italy.
2. ENI SpA, San Donato Milanese, Italy.

## Abstract
Increased concentrations of greenhouse gases in the atmosphere are known to be the main cause of global warming. Among the various decarbonisation strategies proposed, geological storage of $CO_2$ is one of the most interesting options for reducing net carbon emissions to the atmosphere. The safe long-term storage of $CO_2$ in spatially confined underground volumes requires the combination of a reservoir and an undamaged structural trap with a suitable low-permeability caprock, such as is potentially provided by deep saline aquifers, depleted oil and gas fields and unminable coal seams. In order to prevent CO2 leakage to the atmosphere over long geological time scales, the potential caprock alterations due to contact with CO2 need to be considered. In particular, CO2 dissolution and diffusion in the pore fluid leads to acidification of the in-situ brine, causing chemical reactions with some caprock minerals and potentially affecting mechanical and transport properties.
This paper presents a reactive transport model to assess the effects of pore water acidification on caprock materials. The model includes the water mass balance equation for the saturated porous medium and the mass balance equation for all primary chemical species dissolved in water, following the theoretical approach presented in Steefel & Lasaga (1994). The proposed modelling approach considers both the aqueous (homogeneous) reactions of $CO_2$ dissolved in water (assumed to be in equilibrium) and the dissolution kinetics of calcite in the acidic environment induced by $CO_2$ injection. Calcite dissolution is finally coupled to porosity changes via the reactive surface area of the mineral and the reaction rate. The chemo-hydraulic coupling is addressed by considering porosity changes in the storage term of the balance equations and by introducing an appropriate link between hydraulic conductivity and current porosity.
**Keywords:** Geological carbon storage; reactive transport; calcite dissolution, chemo-hydraulic coupling

## Introduction
Increased concentrations of greenhouse gases in the atmosphere are known to be the primary cause of global surface temperature rise and, consequently, climate change [1]. In order to limit global warming, several decarbonisation strategies have been proposed: among them, geological $CO_2$ storage is one of the most promising short- to medium-term options for significantly improving $CO_2$ sinks and reducing net carbon emissions to the atmosphere.
The safe long-term storage of $CO_2$ in underground geological structures requires the combination of a reservoir and of a caprock (seal), i.e. a structural trap characterized by structural integrity and a suitable low permeability. For these reasons, deep saline aquifers, depleted oil and gas fields and unminable coal seams are thus the primary targets for the underground storage of supercritical $CO_2$. The occurrence of natural reservoirs implies that certain lithotypes have a sealing capacity that can prevent leakage of gas to the atmosphere over long geological time periods (i.e. millions of years); however, in order to assess the risk of $CO_2$ leakage through caprock above storage sites, the potential caprock alterations due to the contact with $CO_2$ must be considered. In fact, although certain caprocks can be suitable for hydrocarbons over geological time periods, $CO_2$ in contact with the seal may pose additional risks, to be evaluated. As for natural hydrocarbon accumulation, shales and evaporites are potential seals also for carbon storage. With particular reference to shales, their mechanical and transport properties are not only controlled by the behaviour of clay minerals [2,3,4], but $CO_2$ dissolution and diffusion in water also result in acidification of the in situ brine, potentially causing chemical reactions with some minerals and consequently affecting the mechanical and transport properties [5].
This work presents a reactive transport model to assess the effects of pore water acidification on geological materials. The model includes the water mass balance equation for the saturated porous medium and the mass balance equation for all the primary species dissolved in water, according to the theoretical approach presented in [6]. The model accounts for both the aqueous (homogeneous) reactions of the $CO_2$ dissolved in water (assumed to be in equilibrium) and the dissolution kinetics of calcite in the acidic environment induced by $CO_2$ injection. Calcite dissolution is finally linked to porosity changes via the reactive surface area of the mineral and the reaction rate. Chemo-hydraulic

coupling is addressed by considering porosity changes in the storage term of the balance equations and by introducing a suitable link between hydraulic conductivity and current porosity. The model requires the solution of an initial chemical speciation problem, and then the integration of a set of partial differential equations (the mass balance equations of water and of the master primary species dissolved in water) and non-linear algebraic equations (to obtain the concentration of all the chemical species involved), which in this study has been performed via the Finite Element software Comsol Multiphysics ®, according to the approach presented in [7]. The numerical model has been validated according to the numerical benchmark proposed in [8], developed to reproduce a geochemical scenario where mineral dissolution causes permanent alterations in the transport properties of a porous medium.

## Theoretical framework and model equations

This section briefly summarizes the equations for the numerical simulations of the chemo-hydraulic response of caprock materials upon acid injection.

**Mass balance, equilibrium and kinetics equations**

To identify the geochemical interaction between dissolved $CO_2$ and the porous medium, a solute mass balance equation for all the $N$ chemical species involved in the problem must be in principle considered. By assuming, for the sake of simplicity, the porous medium as water-saturated, the solute mass balance equation for a chemical species $i$ dissolved in the aqueous phase of the porous medium can be written as [9]:

$$\frac{\partial \phi c_i}{\partial t} + \nabla \cdot (\boldsymbol{q} c_i + \phi \boldsymbol{D} \nabla c_i) + R_i = 0 \qquad \text{Eq. 1}$$

where $\phi$ is the porosity [-], $t$ is time [s], $c_i$ [mol/m$^3$] is the mass concentration of the aqueous chemical species $i$, expressed in terms of units of moles per unit volume solution. Both advection and hydrodynamic dispersion are considered in the divergence term, being $\mathbf{q}$ the specific discharge per unit area of the porous medium (i.e., Darcy velocity) and $\mathbf{D}$ [m/s$^2$] is the hydrodynamic dispersion tensor. The hydrodynamic dispersion tensor accounts for both diffusion and mechanical dispersion process:

$$\boldsymbol{D} = D_p \boldsymbol{I} + \alpha_T |\mathbf{v}| \boldsymbol{I} + (\alpha_L - \alpha_T) \frac{\mathbf{v}^\mathbf{T}\mathbf{v}}{|\mathbf{v}|} \qquad \text{Eq. 2}$$

where $D_p$ [m/s$^2$] is the diffusion coefficient, $\alpha_L$ and $\alpha_T$ [m] are the longitudinal and transversal dispersion coefficients and $\mathbf{v}$ [m/s] the real pore fluid velocity (i.e. the Darcy velocity divided by porosity). The source/sink term $R_i$ [mol/(m$^3$ s)] is the total reaction rate of species $i$ in solution, expressed in terms of moles per unit total volume per unit time. Conventionally, the reaction term can be split into dissolution-precipitation (heterogeneous) reactions $R_i^{min}$ and aqueous (homogeneous) reactions, $R_i^{aq}$. If chemical equilibrium between aqueous species is assumed, it is convenient, from the numerical point of view, to reduce the number of independent concentrations. In particular, in a system containing $N$ aqueous species, the number of independent chemical components $N_p$ (primary species) is reduced from $N$ by the $N_s$ linearly independent chemical reactions:

$$N_p = N - N_s \qquad \text{Eq. 3}$$

In the following, $c_\alpha$ (with $\alpha$ ranging from 1 to $N_p$) then refers to the $N_p$ primary species, while $c_\beta$ ($\beta$ ranging from 1 to $N_s$) refers to the $N_s$ secondary species.

**Homogeneous reaction term**

The reversible chemical reactions between the primary and the secondary species take the classical form of equilibrium chemical reactions:

$$A_\beta \rightleftharpoons \sum_{\alpha=1}^{N_p} \nu_{\beta\alpha} A_\alpha \qquad \text{Eq. 4}$$

where $A_\beta$ and $A_\alpha$ are chemical formulas of the secondary species $\beta$ and of the $N_p$ primary species $\alpha$, and $\nu_{\beta\alpha}$ is the stoichiometric coefficient of the primary species $\alpha$ in a reversible aqueous reaction with the secondary species $\beta$. The reversible reactions provide an algebraic link between the primary and secondary species, via the law of mass action for each reaction. For instance, in a general reaction with A, B, C and D components and $a$, $b$, $c$ and $d$ stoichiometric coefficient:

$$aA + bB \leftrightarrow cC + dD \qquad \text{Eq. 5}$$

in a homogeneous equilibrium, the law of mass action reads:

$$K = \frac{{a_C}^c {a_D}^d}{{a_A}^a {a_B}^b} \qquad \text{Eq. 6}$$

where $a_A$, $a_B$, $a_C$ and $a_D$ are the activities of the components of the reaction and $K$ is the equilibrium constant. Accordingly, the activity $a_{s\beta}$ of the secondary species $\beta$ is related from the quantitative point of view to the activities $a_{p\alpha}$ of the primary species $\alpha$ via the law of mass action for each reaction as:

$$K_{eq,\beta} = a_{s\beta} \prod_{\alpha=1}^{N_p} {a_{p\alpha}}^{\nu_{\beta\alpha}} \qquad \text{Eq. 7}$$

which can be rewritten in the logarithmic form as:

$$log a_{s\beta} = log K_{eq,\beta} + \sum_{\alpha=1}^{N_p} \nu_{\beta\alpha} \, log a_{p\alpha} \qquad \text{Eq. 8}$$

The chemical activities $a_{p\alpha}$ and $a_{s\beta}$ [-] are in general defined as:

$$a = \gamma \frac{c}{c^\theta} \qquad \text{Eq. 9}$$

where $c^\theta$ is a standard concentration equal to 1 mol/l and $\gamma$ [-] is the activity coefficient, linking activity and concentration.

**Heterogeneous reaction term**

The heterogeneous reaction term $R_\alpha^{min}$ is the sum of all the individual mineral dissolution-precipitation reactions that involve the species $\alpha$ (and thus affect its concentration) and reads:

$$R_\alpha^{min} = \sum_{m=1}^{N_m} \nu_{m\alpha}\, r_m A_m \qquad \text{Eq. 10}$$

where $r_m$ $\left[\frac{\text{mol}}{\text{m}^2\text{s}}\right]$ is the rate of precipitation/dissolution of mineral $m$ per unit area of the mineral $m$, $A_m$ $\left[\frac{\text{m}^2}{\text{m}^3}\right]$ is reactive surface area (area of the solid constituents per total unit volume) and $\nu_{m\alpha}$ is the stoichiometric coefficient of the species $\alpha$ in the dissolution-precipitation reaction considered (i.e. the number of moles of $\alpha$ in m). According to the rate law based on transition state theory and assuming that transport does not play any role on the dissolution/precipitation rate (i.e., surface-controlled dissolution rate), the overall rate of dissolution or precipitation for a mineral $m$ is:

$$r_m = k_{+,m} \prod_i a_i^{n_i} \left(1 - \frac{Q_m}{K_{eq,m}}\right) \qquad \text{Eq. 11}$$

in which $k_{+,m}$ $\left[\frac{mol}{m^2 s}\right]$ represents the forward rate constant, $a_i$ is the activity of an inhibiting or catalyzing species raised at the power of $n_i$, $Q_m$ [-] is the ion activity product and $K_{eq,m}$ [-] is the equilibrium constant for the mineral-water reaction written as the destruction of one mole of $m$. The ratio $\frac{Q_m}{K_{eq,m}}$ represents the reprecipitation fraction of the mineral. The index $i$ varies from 1 to $N_p$+$N_m$. The ion activity product $Q_m$ [-] can be finally written as:

$$Q_m = \prod_{\alpha=1}^{Np} a_\alpha{}^{\nu_{m\alpha}} \qquad \text{Eq. 12}$$

in which the activities $a_\alpha$ of $N_p$ primary species $\alpha$ with exponent equal to their stoichiometric coefficient $\nu_{m\alpha}$ are multiplied.

**Liquid phase mass balance equation**

The velocity vector that appears in the advection term of the solute mass balance equations (Eq. 1) can be evaluated via the liquid phase balance equation, that in the case of a saturated porous medium can be expressed as:

$$\frac{\partial \phi}{\partial t} + \frac{\phi}{\rho^l}\frac{\partial \rho^l}{\partial p}\frac{\partial p}{\partial t} + \nabla \boldsymbol{q} + Q_p = 0 \qquad \text{Eq. 13}$$

where $\phi$ is the porosity [-], $t$ is the time [$s$], $\rho^l$ $\left[\frac{\text{Kg}}{\text{m}^3}\right]$ is the fluid density, $p$ [Pa] is the fluid pressure, $\boldsymbol{q}$ [m/s] is the Darcy velocity vector in the hypothesis of laminar flow (i.e. specific discharge, per unit area of the porous medium), $Q_p$ [1/s] is the source-sink term. The Darcy velocity vector $\boldsymbol{q}$ depends on the hydraulic pressure gradient via the Darcy law:

$$\boldsymbol{q} = -\frac{k}{\mu}(\nabla p - \rho^l \boldsymbol{g}) \qquad \text{Eq. 14}$$

being $\mu$ [Pa*s] the water dynamic viscosity, $k$ [m$^2$] the intrinsic permeability and $\boldsymbol{g}$ the gravity vector [m/s$^2$]. By considering the interaction between the chemical species dissolved in water and the rock-solid matrix, porosity $\phi$ is linked not only to pressure $p$ (i.e., poro-mechanical effects), but also to reaction kinetics as:

$$\frac{\partial \phi}{\partial t} = \frac{\partial \phi}{\partial p}\frac{\partial p}{\partial t} + \sum_{m=1}^{N_m} A_m r_m V_{m,n} \qquad \text{Eq. 15}$$

The chemical reaction kinetics term (...) is given by the product of the reactive surface area $A_m$ $\left[\frac{\text{m}^2}{\text{m}^3}\right]$, the dissolution rate $r_m$ $\left[\frac{\text{mol}}{\text{m}^2\text{s}}\right]$ and the molar volume $V_m$ $\left[\frac{\text{m}^3}{\text{mol}}\right]$ of the minerals $m$ composing the solid phase. Substituting Eq. 15 in Eq. 13, the fluid mass balance equation is often rewritten as:

$$S_s \frac{\partial p}{\partial t} + \nabla \boldsymbol{q} + Q_p + \sum_{m=1}^{N_m} A_m r_m V_{m,n} = 0 \qquad \text{Eq. 16}$$

where $S_s$ [1/Pa] is the specific storage term, which reads $S_s = \frac{\partial \phi}{\partial p} + \frac{\phi}{\rho^l}\frac{\partial \rho^l}{\partial p}$, and accounts for porous matrix deformation due to pore pressure changes and for fluid compressibility. Since chemical reactions are typically much slower than liquid fluid transport, the kinetics reaction term are often neglected in the fluid mass balance equation. Vice versa, porosity changes induced by geochemical reactions mainly affects fluid flow via possible alteration of the intrinsic permeability $k$. In this work, the link between porosity and permeability is provided by the Kozeny-Carman relationship:

$$k = k_0 \left(\frac{\phi}{\phi_0}\right)^2 \left(\frac{1-\phi_0}{1-\phi}\right)^3 \qquad \text{Eq. 17}$$

where $k_0$ is a scalar parameter, corresponding to the permeability coefficient for $\phi = \phi_0$.

**Boundary conditions for the reactive transport problem**

Dirichlet and Neumann boundary conditions are adopted in reactive transport problems on the boundary of the domain $\Gamma$, as:

$$\begin{aligned} p &= \overline{p} \; on \; \Gamma_{D,}^{p} \\ -\boldsymbol{q} \cdot \boldsymbol{n} &= \overline{q} \; on \; \Gamma_{N,}^{p} \\ c_{T\alpha} &= \overline{c}_{T\alpha} \; on \; \Gamma_{D,}^{\alpha} \\ -(\boldsymbol{q} c_{T\alpha} - \phi \boldsymbol{D} \nabla c_{T\alpha}) \cdot \boldsymbol{n} &= \overline{J}_\alpha \; on \; \Gamma_{N,}^{\alpha} \end{aligned} \qquad \text{Eq. 18}$$

$\overline{p}$ [Pa] and $\overline{c}_{T\alpha}$ $\left[\frac{mol}{m^3}\right]$ are the prescribed hydraulic pressure and total concentration of the primary species $\alpha$ at the boundary where the Dirichlet constraints apply, $\overline{q}$ [m/s] and $\overline{J}_\alpha$ $\left[\frac{mol}{m^2 s}\right]$ are the seepage velocity and total mass flux, and $\mathbf{n}$ is the outward unit vector normal to the boundary $\Gamma_N$ where Neuman (i.e. flux) boundary conditions are applied.

## Validation with a numerical and experimental benchmark

In the following, the numerical approach introduced in the previous section for the solution of the reactive

transport problem is validated by performing a numerical simulation of calcite dissolution due to the injection of sulphuric acid, together with the related porosity and permeability changes. [8] performed a flow-through column numerical analysis: the cylindrical reactor is 0.07 m height, with an inner diameter of 0.0099 m. One sand-calcite mixture layer is packed between two layers of quartz sand placed on the top and bottom of the cylinder (Fig. 1). The packing layers are 0.024 m, 0.022 m, and 0.024 m respectively. The calcite-containing interlayer is made by combining quartz sand (quartz volume fraction $\phi_0^{quartz} = 0.456$) and calcite grains (calcite volume fraction $\phi_0^{calcite} = 0.2185$) in a 2:1 weight ratio. At the beginning of the test, the porous medium is fully saturated. A 0.005 M sulfuric acid solution (pH=2.128) is then injected. The hydraulic inflow occurs at constant volumetric flow rate of $1.67 \cdot 10^{-10}\ m^3/s$, corresponding to a Darcy flow rate equal to $2.1695 \cdot 10^{-6}\ m/s$, while the downstream pore pressure is set equal to 10 kPa (i.e. coincident with the initial pressure in the whole specimen). The entire flowthrough column experiment lasts for 400 hours.

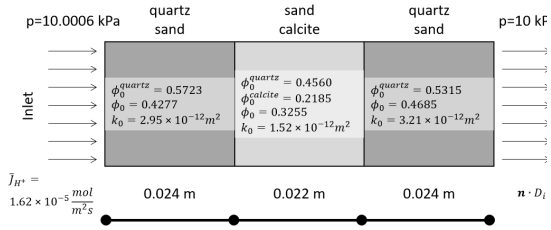


*Fig. 1: Schematic overview of the flow-through experiment along with transport properties of each packing layer (modified after [8])*

Calcite dissolution is accounted for according to the following reaction pathway ([8], [11]):

a. $CaCO_3 + H^+ \rightleftharpoons Ca^{2+} + HCO_3^-$

b. $CaCO_3 + H_2CO_3^* \rightleftharpoons Ca^{2+} + 2HCO_3^-$ Eq. 19

c. $CaCO_3 \rightleftharpoons Ca^{2+} + CO_3^{2-}$

The transition state theory based on kinetics rate law is adopted for the calcite dissolution rate (Palandri and Kharaka, (2004), Molins er al., (2017)):

$$r_{CaCO_3} = \left(k^{acid} a_{H^+} + k^{neutral} + k^{carb} a_{H_2CO_3^*}\right) \cdot \cdot \left(1 - \frac{a_{Ca^{2+}} a_{CO_3^{2-}}}{K_{eq,calc}}\right) \quad \text{Eq. 20}$$

where $k^{acid}$, $k^{neutral}$, $k^{carb}$ $[mol/(m^2 s)]$ are empirical specific dissolution rates which depend on temperature and $K_{eq,calc}$ is the equilibrium constant of calcite dissolution in water ($10^{-8.49}$).
The change in volume fraction of calcite is therefore computed as:

$$\frac{d\phi^{CaCO_3}}{dt} = -r_{CaCO_3} * S_{CaCO_3} * V_{m,CaCO_3} * \phi_{CaCO_3} \quad \text{Eq. 21}$$

From this expression, the porosity of the calcite-rich material is obtained as (under the assumption of negligible volumetric strain):

$$\phi = 1 - \sum_{m=1}^{N} \phi^m \quad \text{Eq. 22}$$

where $\phi^m$ are the volume fraction of the solid constituents:

$$\phi^m = \frac{V^m}{V^{TOT}} \quad \text{Eq. 23}$$

In this study, the solid constituents are the non-reactive quartz component and the reactive calcite, so that:

$$\phi = 1 - \phi^{non-reac} - \phi^{CaCO_3} \quad \text{Eq. 24}$$

Then, if it is assumed that only calcite volume can evolve due to dissolution-precipitation reactions, the porosity of the material evolves according to:

$$\frac{d\phi}{dt} = -\frac{d\phi^{CaCO_3}}{dt} \quad \text{Eq. 25}$$

The numerical results of the model completely implemented in COMSOL Multiphysics® are compared to the solution proposed by [8]. The same set of parameters and of equations for the chemo-hydraulic properties are adopted (see ***Table 1***.)

***Table 1****: Hydraulic and chemical model parameters.*

| Parameter | Symbol and unit | Value |
|---|---|---|
| Diffusion coefficient | $D_p$ [m²/s] | $10^{-9}$ |
| Molar volume calcite | $V_{m,CaCO_3}$ [mol/m³] | $3.693*10^{-5}$ |
| Specific dissolution rates | $k_{acid}$ [mol/m2/s] | 0.50119 |
| | $k_{neutral}$ [mol/m²/s] | $1.55*10^{-6}$ |
| | $k_{carbonate}$ [mol/m²/s] | $3.31*10^{-4}$ |
| Specific surface area | $S_{CaCO_3}$ [m2/m3] | 20 |
| Dynamic viscosity | $\mu$ [Pa s] | $10^{-3}$ |
| Fluid density | $\rho^l$[Kg/m³] | $10^3$ |
| Longitudinal dispersivity | $\alpha_L$ [m] | $10^{-4}$ |

The numerical model implemented in COMSOL Multiphysics consists in a one-dimensional column, subdivided in 1493 quadratic finite elements, with $4.69*10^{-5}$ m maximum length (1024 elements for the two quartz sand layers, 496 for the sand-calcite one). Mass balance equations (Eq. 1) are solved for the selected primary species, namely $H^+$, $SO_4^{2}$ and $Ca^{2+}$ (related to the calcite presence):

$$\frac{\partial \phi c_{TH^+}}{\partial t} + \nabla \cdot (\boldsymbol{q} c_{TH^+} + \phi \boldsymbol{D} \nabla c_{TH^+}) + R_{H^+}^{min} = 0 \quad \text{Eq. 26}$$

$$\frac{\partial \phi c_{TSO_4^{2-}}}{\partial t} + \nabla \cdot \left(\boldsymbol{q} c_{TSO_4^{2-}} + \phi \boldsymbol{D} \nabla c_{TSO_4^{2-}}\right) + R_{SO_4^{2-}}^{min} = 0$$

$$\frac{\partial \phi c_{TCa^{2+}}}{\partial t} + \nabla \cdot \left(\boldsymbol{q} c_{TCa^{2+}} + \phi \boldsymbol{D} \nabla c_{TCa^{2+}}\right) + R_{Ca^{2+}}^{min} = 0$$

The electroneutrality condition is applied for the calculation of the concentration of the primary species $CO_3^{2-}$:

$$c_{CO_3^{2-}} = \frac{1}{z_{CO_3^{2-}}} \sum_{i=1}^{N} c_i z_i \qquad \text{Eq. 27}$$

Initial water composition considers pH=7, namely $c_{TH+}$=$10^{-7}$ mol/l. Calcium, carbon and sulfur species initial values are set low, but not equal to zero to assure numerical stability at the beginning of the simulation ($c_{TCa2+} = c_{TCO32-} = 10^{-13}$ mol/L and $c_{TSO42-} = 5*10^{-9}$ mol/L). Reversible aqueous reactions (Eq. 4) are considered to define the secondary species as function of primary species. The heterogeneous reaction term for each primary species is evaluated according to Eq. 11. The activities of the primary species are calculated via Eq. 9, while the activities of the secondary species are given via Eq. 8. Finally, the updated porosity is obtained after the evaluation of calcite volume fraction evolution (Eq. 22 to Eq. 25).

As for the boundary conditions, sulfuric acid injection is modelled considering an inlet flux of $H^+$ and $SO4^{2-}$ ions on the left side of the domain, calculated accounting for the resulting solution pH=2.128 and the Darcy velocity equal to $2.1695 \cdot 10^{-6}\, m/s$. Dirichlet boundary conditions are imposed at the inlet and outlet sides of the sample for the hydraulic model (Fig. 1). A semipermeable membrane for ions is assumed on the right (outlet) side of the sample.

Fig. 2 shows the comparisons between the prediction of the numerical model and both the benchmark model and experimental results, in terms of calcium and sulphur breakthrough curves. Numerical results compare well the experimental data, especially with respect to sulphur concentration.

Fig. 3 presents the comparisons between the benchmark numerical simulation of [8] and the current analysis in terms of Calcite volume fraction, permeability and porosity distribution at a given time (400 h since the beginning of the injection). Both models are able to reproduce the calcite dissolution due to pore water acidification, in which ion $H^+$ activity plays a major role. As soon as the acidification front proceeds, calcite volume fraction reduces, together with a porosity increase and since porosity dependent permeability model was adopted, permeability increases as a consequence.

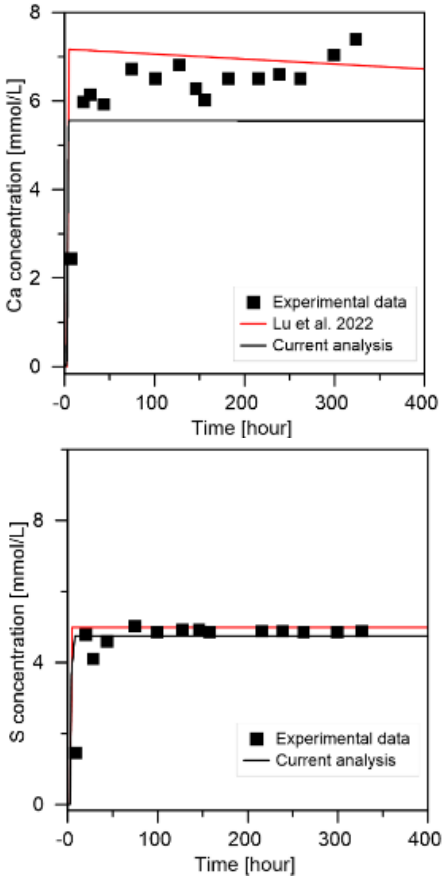


*Fig. 2: Comparison between numerical predictions (current analysis and [8]) and experimental measurements [8]): calcium breakthrough curve and sulfur breakthrough curve.*

## Sensitivity analysis

The model developed has been also used to reproduce the effect of injection of $CO_2$ on the calcite containing materials, as compared with the effects of sulphuric acid. When $CO_2$ is injected in a saturated porous medium, the presence of water leads to a transformation of gaseous $CO_{2(g)}$ in aqueous $CO_{2(aq)}$, i.e. dissolved in the pore water:

$$CO_{2(g)} \rightarrow CO_{2(aq)} \qquad \text{Eq. 28}$$

Part of this aqueous $CO_2$ reacts with water and forms the carbonic acid:

$$CO_{2(aq)} + H_2O \rightarrow H_2CO_3 \qquad \text{Eq. 29}$$

Assuming that $CO_{2(aq)} + H_2CO_3 = H_2CO_3^*$, Eq. 29 can be rewritten as:

$$CO_{2(g)} + H_2O \rightarrow H_2CO_3^* \qquad \text{Eq. 30}$$

The carbonic acid then dissociates in hydrogen and bicarbonate ions:

$$H_2CO_3^* \leftrightarrow H^+ + HCO_3^-, \qquad \text{Eq. 31}$$

In this section, a specimen made of a single calcite layer is considered to present results of some

sensitivity analyses. In particular, a quartz-calcite mixture is considered with initial calcite volume fraction $\phi_0^{calc} = 0.2185$, quartz volume fraction $\phi^{quartz} = 0.456$ and initial porosity $\phi_0 = 0.3255$. The length of the specimen is 0.007 m (Fig. 4). An injection flow rate $Q = 1.67 \cdot 10^{-10}\ m^3/s$ (resulting in a Darcy flow rate $q = 2.1695 \cdot 10^{-6}\ m/s$) is applied at the inlet. At the outlet, a pressure of 0.1 MPa is fixed, while on the left boundary a pressure of 1.0006 MPa is enforced to obtain this Darcy flow rate. The concentration of ions $H^+$ [mol/l] injected in the column is defined through

$$[H^+] = \sqrt{10^{-7.8}\left(P_{CO_2}\right)} \qquad \text{Eq. 32}$$

The concentrations computed via Eq. 32 have the unit of [mol/l]: in order to obtain the inward fluxes in [mol/m$^2$s] that must be introduced in COMSOL as a boundary condition on the left, they must be multiplied by the Darcy flow rate **q**. On the right (outlet) boundary again a semipermeable membrane for ions is assumed The experiment lasts for 200 days, and the model parameters used are the ones listed in Table 1.

Different values of $P_{CO_2}$ are considered in this analysis, ranging from the atmospheric pressure (0.1 MPa) to a typical value of $CO_2$ injection pressure in geological carbon storage applications (7.3 MPa). Of course, a variation in the injection pressure $P_{CO_2}$ corresponds to a variation in the concentration of ions $[H^+]$ injected through the column: the values of $P_{CO_2}$ considered and the corresponding inward fluxes $\bar{J}_{[H^+]}$ are listed in **Table 2**. For increasing values of injection pressure, the concentration of ions $H^+$ increases: accordingly, the calcite volume fraction (Fig. 5b) decreases, while the dissolved calcite increases (Fig. 5a).

***Table 2**: Injection pressure $P_{CO_2}$ and related injected concentration of ions $H^+$*

| $P_{CO_2}$ | $[H^+]$ | $\bar{J}_{[H^+]}$ |
|---|---|---|
| [MPa] | [mol/m$^3$] | [mol/m$^2$s] |
| 0.1 | 0.126 | $2.73 \cdot 10^{-7}$ |
| 1.9 | 0.548 | $1.19 \cdot 10^{-6}$ |
| 3.7 | 0.765 | $1.66 \cdot 10^{-6}$ |
| 5.5 | 0.933 | $2.02 \cdot 10^{-6}$ |
| 7.29 | 1.07 | $2.33 \cdot 10^{-6}$ |

The low percentage of dissolved calcite is due to the low values of $a_{H^+}$ and $a_{H_2CO_3}$, which are related to calcite dissolution. Those activities $a_{H^+}$ and $a_{H_2CO_3}$ increases for increasing values of $P_{CO_2}$, thus inducing larger dissolved calcite. On the contrary, the reprecipitation decreases for increasing values of injection pressure: this reflects also the behaviour in terms of $a_{CO_3^{2-}}$ (decreasing for increasing $P_{CO_2}$). The small increase in calcite dissolution for increasing values of $P_{CO_2}$ is reflected in a very small variation of porosity and, of permeability.

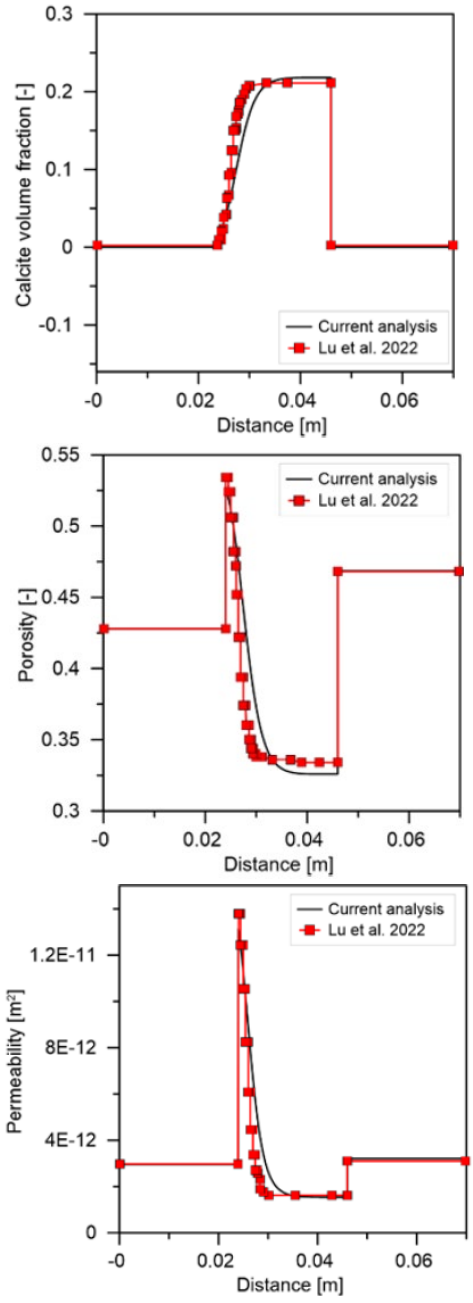


*Fig. 3: Comparison between [8] and current analysis. The curves are evaluated at t=400 h.*

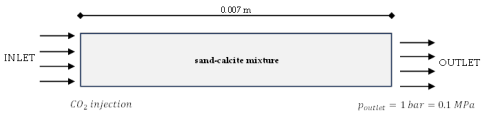


*Fig. 4: Geometry and boundary conditions of the specimen.*

## Conclusions

A numerical model, completely implemented in Comsol Multiphsycs, has been proposed to reproduce the acidification induced by CO2 injection

in porous media, as well as the consequences in terms of evolution of transport properties. A reactive transport model has been implemented and coupled to the pore fluid mass balance equation. The model has been validated with a numerical benchmark developed to reproduce acid injections and then used to perform some sensitivity analyses. The agreement between the two models is satisfactory, despite some slight differences that can be attributed to the different numerical mesh and numerical solver scheme. In the future, the model will be validated with respect to experimental data involving CO2 injection into reservoir materials and coupled with the equilibrium equations, once a suitable constitutive model accounting for acidification-induced damage is implemented in the numerical platform.

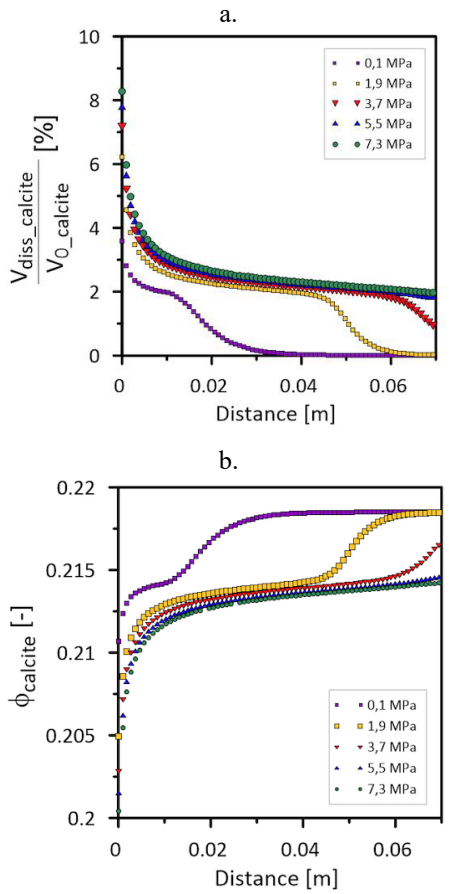


*Fig. 5: Comparison between numerical simulations for injection $CO_2$ at different $P_{CO_2}$ in terms of (a) dissolved calcite percentage; and (b) calcite volume fraction at = 200 days.*

## Acknowledgements

Funding was provided by ENI SpA within the project "ECoPhysiCS". The authors gratefully thank Eni S.p.A. for the authorization to publish this work.

## References

[1] R. Shukla, P. Ranjith, A. Haque and X. Choi, "A review of studies on CO2 sequestration and caprock integrity", *Fuel*, 89 (10), pp. 2651-2664, 2010

[2] G. Scelsi, A.A. Abed, G. Della Vecchia, G. Musso, W. Sołowski, "Modelling the behaviour of unsaturated non-active clays in saline environment", *Engineering Geology*, 295, 106441, 2021.

[3] D.N. Espinoza and J.C. Santamarina, "Clay interaction with liquid and supercritical CO2: The relevance of electrical and capillary forces". *International Journal of Greenhouse Gas Control*, 10, pp. 351-362, 2012.

[4] G. Musso, G. Scelsi and G. Della Vecchia, "Chemo-mechanical behaviour of non-expansive clays accounting for salinity effects", *Géotechnique*, 74(7), pp. 632-646.

[5] L. Gramegna, G. Musso, A. Messori, A. and G. Della Vecchia, "A reactive transport model for calcite-rich caprocks in the context of geological carbon storage". In *Symposium on Energy Geotechnics*, pp. 1-2.

[6] C.I. Steefel and A.C. Lasaga, "A coupled model for transport of multiple chemical species and kinetic precipitation/dissolution reactions with application to reactive flow in single phase hydrothermal systems", *American Journal of science*, 294(5), pp. 529-592, 1994.

[7] R. Lopez-Vizcaino, A. Yustres, V. Cabrera, and V. Navarro, "A worksheet-based tool to implement reactive transport models in COMSOL Multiphysics", *Chemosphere,* 163, 129176, 2001.

[8] R. Lu, T. Nagel, J. Poonoosamy, D. Naumov, T. Fischer, V. Montoya, V., ... & H. Shao, "A new operator-splitting finite element scheme for reactive transport modeling in saturated porous media", *Computers & Geosciences*, 163, 105106, 2022.

[9] G. Della Vecchia, G. Musso, "Some remarks on single-and double-porosity modeling of coupled chemo-hydro-mechanical processes in clays", *Soils and Foundations,* 56(5), pp. 779-789.

[10] L.N. Plummer, T:M:L.Wigley, D.L. Parkhurst, "The kinetics of calcite dissolution in $CO_2$-water systems at 5 ◦ to 60 ◦C and 0.0 to 1.0 atm $CO_2$", *American Journal of Science,* 278, pp. 179–216.